Journal of Arrhythmia 30 (2014) 292–299

Contents lists available at ScienceDirect

Journal of Arrhythmia

journal homepage: www.elsevier.com/locate/joa

Original Article

The morphology of unipolar potentials predicts the depth of activation foci ☆

Yoshiaki Kaneko, MD, PhD*, Tadashi Nakajima, MD, PhD, Masahiko Kurabayashi, MD, PhD

Department of Medicine and Biological Science, Gunma University Graduate School of Medicine, 3-39-22 Showa-machi, Maebashi, Gunma 371-8511, Japan

ARTICLE INFO

Article history:
Received 10 February 2014
Accepted 26 February 2014
Available online 26 April 2014

Keywords:
Epicardial mapping
Epicardial electrogram
Unipolar potential
Intramyocardial pacing
Ventricular pacing
Catheter ablation
Ventricular arrhythmia

ABSTRACT

Background: The depth of an arrhythmic focus is a major determinant of ablation procedural outcome. This study examined the relationship between the morphology of unipolar potentials and the depth and horizontal distance to activation foci.

Methods: Unipolar left ventricular epicardial mapping was performed in 7 open-chest dogs, using silicon sheets with 12 unipolar electrodes 1 mm apart, during bipolar pacing from an octopolar plunge electrode with 1-mm interelectrode spacing. The morphology of the unipolar electrograms was classified as QS, rS, qrS, qRS, rsr'S, or rsR'S.

Results: A QS complex was recorded immediately above a subepicardial or mid-myocardial pacing site. An rS complex was recorded away from a subepicardial pacing site. A positive wave originating from a down sloping deflection (R-in-QR) such as r wave in qrS, R wave in qRS, r′ wave in rsr'S or R′ wave in rsR'S complexes was observed when the recording was above a deep myocardial pacing site or away from a mid-myocardial pacing site. The amplitude of negative wave immediately before R-in-QR (Q-in-QR) was inversely correlated with the horizontal ($R=-0.40$; $P<0.0001$) and linear ($R=-0.22$; $P=0.0006$) distance to the pacing site, and the amplitude of R-in-QR was positively correlated with the horizontal ($R=0.25$; $P=0.0001$) and linear ($R=0.29$; $P<0.0001$) distance to the pacing site. The amplitude of the initial r wave was not correlated with the depth or horizontal and linear distance to the pacing site.

Conclusion: The morphology of unipolar electrograms predicted the horizontal distance and the depth of nearby foci of activation.

1. Introduction

By eliminating the arrhythmogenic focus, catheter ablation can be a curative therapy of ventricular tachyarrhythmias (VTAs). Majority of ablations of VTA that were successful were performed using an endocardial approach because the arrhythmogenic focus, for instance, of idiopathic ventricular tachycardia originating from the outflow tract, is located near the endocardium. However, ablation of a subset of intramural or epicardial origin ventricular tachycardias from the endocardium may be challenging [1–4]. The depth of the arrhythmogenic focus or the perpendicular distance between the focus and the endocardial site of ablation is a major determinant of successful ablation procedures. Activation maps of intracardiac bipolar potentials recorded during on-going ventricular tachycardia can identify the site of earliest activation of the endocardial surface in contact with the tip of the catheter, although they do not clearly indicate whether the focus is endocardial, mid-myocardial or epicardial. In contrast, unipolar potentials, which can be recorded to locate accessory pathways or the origin of some tachyarrhythmias [5–15], also reflect the activation of sites located away from the recording surface [16,17]. We conducted this experimental study to examine the relationship between the morphology of unipolar potentials and the depth and horizontal distance of activation foci.

2. Methods

2.1. Animal preparation

We used 7 healthy, adult mongrel dogs weighing 9–13 kg (mean, 12.4 ± 1.2 kg) for this study. They were anaesthetized with 30 mg/kg of pentobarbital sodium, intubated, and ventilated with a respirator (Harvard Apparatus, South Natick, MA) at a rate of 15–18 cycles/min

Abbreviations: Q-in-QR, negative wave immediately before R-in-QR defined as follows; R-in-QR, positive wave originating from a down sloping deflection immediately before the minimum d*V*/d*t*; VTA, ventricular tachyarrhythmia

☆This study was presented in a 'Featured Poster' session of the 31st annual scientific meeting of the Heart Rhythm Society held in Denver, USA, on 12 May 2010.

* Corresponding author. Tel.: +81 27 220 8145; fax: +81 27 220 8158.
E-mail address: kanekoy@gunma-u.ac.jp (Y. Kaneko).

http://dx.doi.org/10.1016/j.joa.2014.02.009
1880-4276/

and volume of 15–20 mL/kg, adjusted to maintain the arterial pH at 7.35–7.45, PCO_2 at 35–45 mmHg and PO_2 at >80 mmHg. Left thoracotomy was performed in the fourth intercostal space, and the heart was suspended in a pericardial cradle. To record unipolar electrograms at multiple epicardial sites during ventricular pacing from multiple intramural locations, we designed and manufactured a silicon sheet with 12 surface button electrodes (Unique Medical, Inc., Tokyo, Japan), 1 mm apart, for the recording of unipolar electrograms, and an octopolar plunge electrode with a 1-mm interelectrode separation for bipolar pacing (Fig. 1). The sheet was applied to the epicardial surface of the left anterolateral wall, and its edges were sutured to the pericardium. The plunge electrode was inserted near the most proximal unipolar recording site on the edge of the sheet, taking care to avoid injuries to the epicardial arteries. The needle was introduced from the left ventricular epicardial surface, such that the distal electrode was near the endocardium and the most proximal pacing bipole was at a depth of 1 mm from the epicardial surface. The sheet was moistened with saline to optimize electrical contact of the electrodes with the myocardium. Following creation of complete atrioventricular block by a transseptal injection of ethanol [18], the ventricular rate was controlled by pacing from any plunge electrode at a cycle length of 600 ms. The output was set just above the myocardial capture threshold to minimize the amplitude of the pacing artefact. The unipolar recording electrodes were connected to the anodal (positive) input of the amplifier, each referenced to a Wilson central terminal.

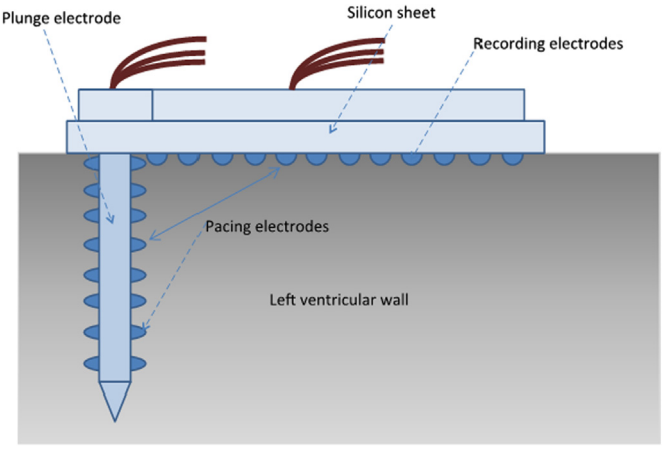

Fig. 1. Schematic representation of the silicon sheet used to record unipolar electrograms and the octopolar plunge electrode used for bipolar pacing from various depths of the left ventricular wall. The bidirectional arrow illustrates the linear distance between the 4-mm depth of the pacing site and the 5-mm recording site, calculated as $\sqrt{4^2+5^2}$.

2.2. Data acquisition and analysis

Unipolar electrograms were recorded from the sheet electrode during regular ventricular pacing from each bipole of the plunge electrode. The electrograms were amplified and filtered between 0.05 and 500 Hz, using a polygraph 366 multichannel data acquisition system (Sanei Denki Co., Ltd., Kyoto, Japan), and recorded at a 100-mm paper speed. The first derivative (dV/dt) of each unipolar electrogram was simultaneously recorded to

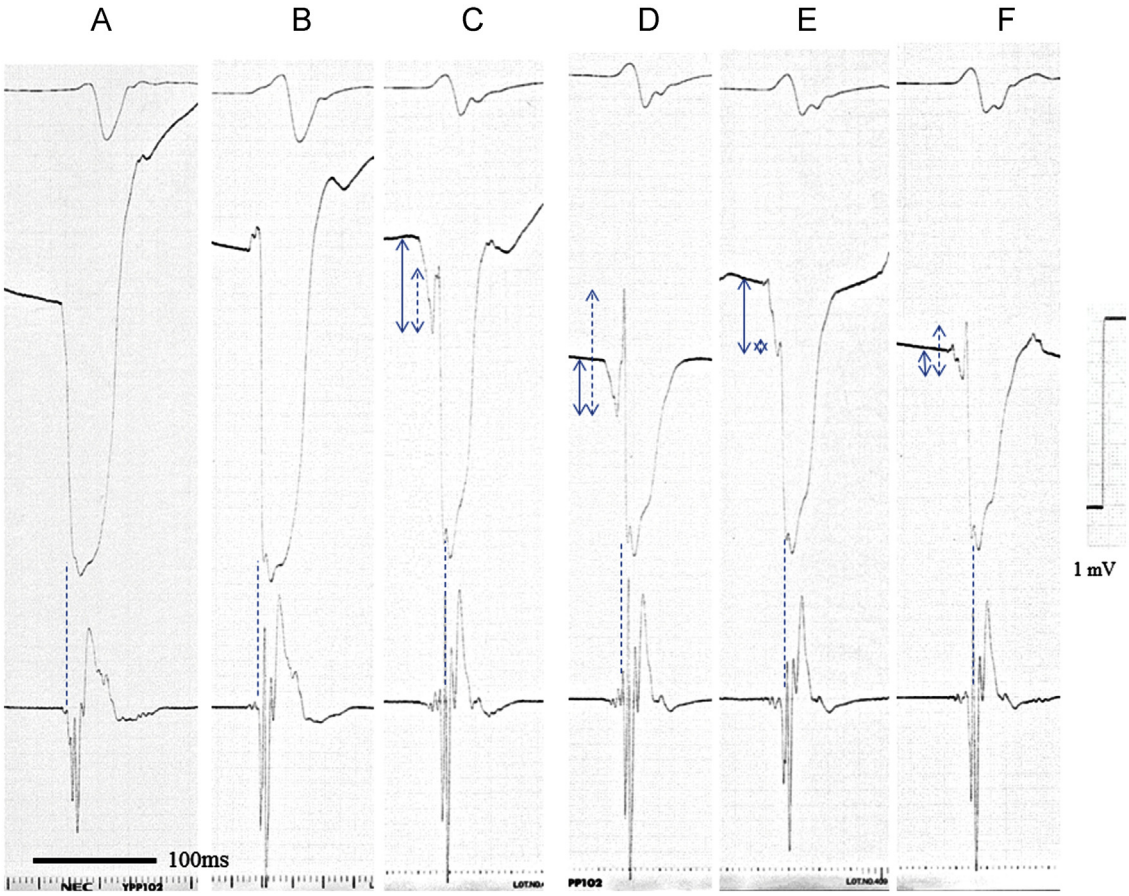

Fig. 2. Representative examples of surface QRS (upper tracing), unipolar electrograms (middle tracing) showing QS (A), rS (B), qrS (C), qRS (D), rsr'S (E) and rsR'S (F) patterns and the first derivative (d*V*/d*t*) of each unipolar electrogram (lower tracing). The dashed lines indicate the timing of the minimum d*V*/d*t*. Bidirectional (a) straight and (b) dashed arrows indicate (a) the amplitude of q in qrS or qRS (B or C) or s in rsr'S or rsR'S (E or F), and (b) the amplitude of r in rS or qrS (B or C), r' in rsr'S (E), R in qRS (D) or R' waves in rsR'S (F), respectively. See text for further explanation.

determine the timing of the minimum dV/dt corresponding to the precise local activation beneath the recording site (Fig. 2). A total of 490 unipolar electrograms were analyzed. The depth of the pacing site was the distance between the pacing site and the epicardial surface. The horizontal distance of the recording site was the space between the recording unipole and the epicardial insertion of the plunge electrode. The linear distance between pacing and the recording sites was measured between the depth of the pacing site and the recording site.

The morphology of the unipolar potentials was visually classified into 6 patterns of QS, rS, qrS, qRS, rsr'S or rsR'S depending on the presence or absence of (1) an initial, monophasic, or multiphasic r wave, and (2) a positive deflection originating from the descending slope immediately before the timing of the minimum d*V*/d*t* (R-in-QR), expressed as *r* or *r*′ when its peak was below the baseline, or R or R′ when its peak was above the baseline (Fig. 2). When the pacing artefact was visible, the presence or absence of an initial r wave was ascertained by visually subtracting a non-propagated artefact from the initial component of the electrogram. The amplitude of the unipolar potentials was measured between their maximum positive and maximum negative peaks, and the amplitude of negative waves occurring immediately before the R-in-QR (Q-in-QR), such as a q wave in qrS or qRS or an s wave in rsr'S or rsR'S complexes, was measured between their baseline and peak, and the amplitude of R-in-QR waves such as an r wave in qrS, R wave in qRS, r′ wave in rsr'S, or R′ wave in rsR'S complexes was measured between the onset and peak of each wave (Fig. 2).

2.3. Statistical analysis

Continuous variables are expressed as means ± SD. Between-pattern differences were examined by one-way analysis of variance, followed by Tukey's test. The presence versus absence of correlations was confirmed by simple linear regression analysis. A P value < 0.05 was considered statistically significant. The data were analyzed using the Ekuseru–Toukei 2012 Excel statistical software package (Social Survey Research Information Co., Ltd., Tokyo, Japan).

3. Results

3.1. Representative example

Recordings of unipolar potentials in a single dog are shown in Figs. 3, 4, and 5. During subepicardial pacing, a QS pattern was observed near the pacing site (Fig. 3A–C), whereas an rS pattern was observed away from the pacing site, with the r wave widening proportionally to the distance from the pacing site (Fig. 3D–J).

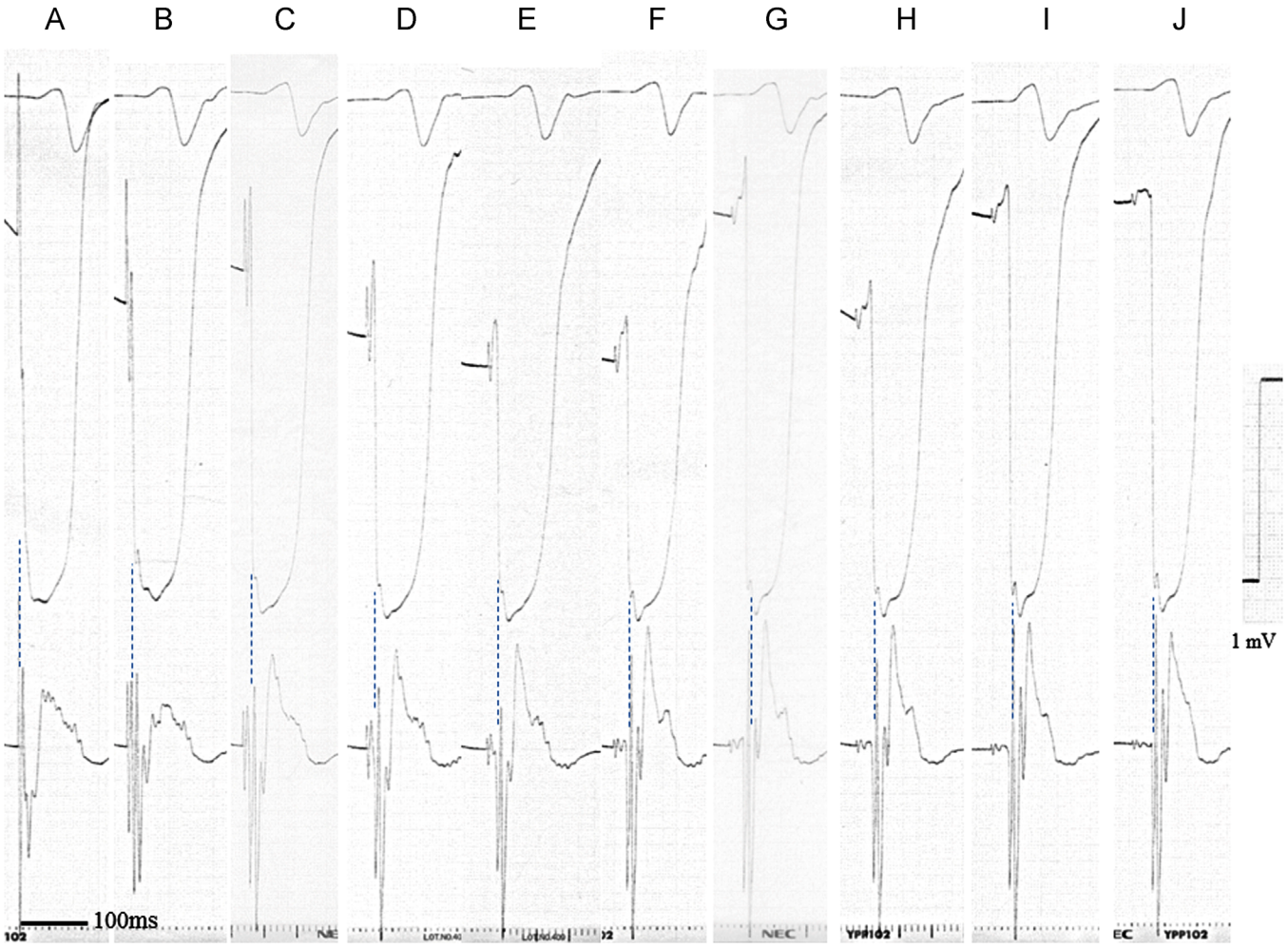

Fig. 3. Representative examples of unipolar electrograms (middle tracing) recorded at a 1–10 mm distance (panels A–J) during pacing from a bipole set at a depth of 0 mm below the epicardial surface, recorded along with the surface electrocardiogram (upper tracing) and the first derivatives (d*V*/d*t*) of each unipolar electrogram (lower tracing). The unipolar potentials recorded at 1–3-mm and 4–10-mm distances show QS (panels A and C) and rS (panels D–J) patterns, respectively. The amplitude of the pacing artefact, visible at the onset of each unipolar potential, decreases in proportion to the distance between the pacing and recording sites. Note that no positive wave is present in the descending slope of the unipolar potentials. The dashed lines indicate the timing of the minimum d*V*/d*t*. See text for further explanation.

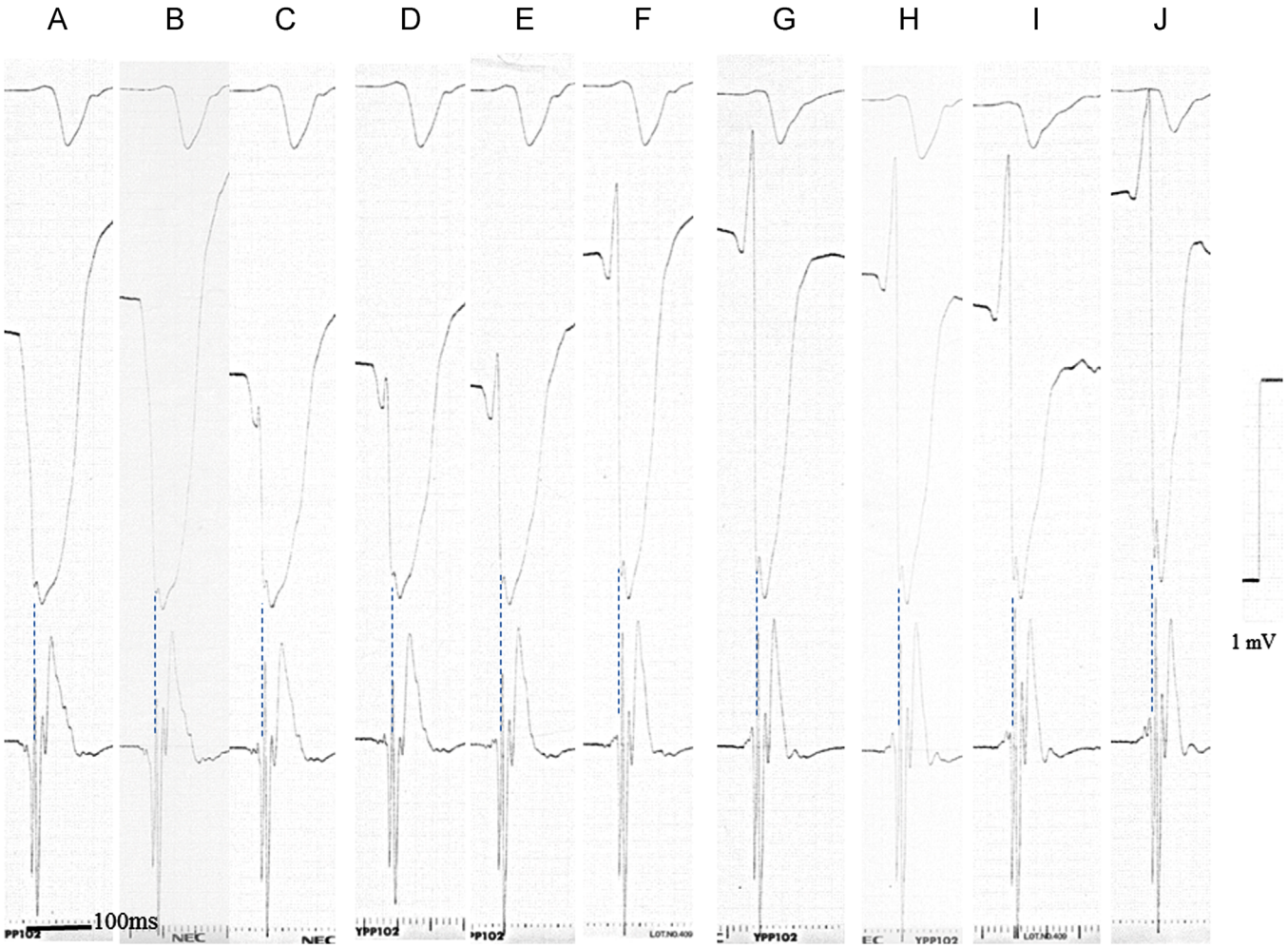

Fig. 4. Representative examples of unipolar electrograms (middle tracing) recorded at 1–10 mm distance (panels A–J) during pacing from a bipole set at a depth of 4 mm under the epicardial surface, recorded along with the surface electrocardiogram (upper tracing) and the first derivatives (d*V*/d*t*) of each unipolar electrogram (lower tracing). The unipolar electrograms recorded at depths of 1–2, 3–4, and 5–10 mm, appear as QS (A and B), qrS (panels C–D) and qRS (panels E–J) complexes. The dashed lines indicate the timing of the minimum d*V*/d*t*. See text for further explanation.

During mid-myocardial pacing, a QS pattern was observed near the pacing site (Fig. 4A and B), with the downward slope becoming shallow proportionally to the distance from the pacing site, and qrS and qRS patterns developing away from the pacing site (Fig. 4C–J). The q wave amplitude decreased, whereas the *r* or *R* wave amplitude increased proportionally to the distance from the pacing site. When recorded at a fixed site adjacent to the insertion site of the plunge electrode, a QS pattern was observed during epicardial (at a depth of 1 mm) or mid-myocardial (at a depth of 5 mm) pacing (Fig. 5A–E). The descending slope became shallow in proportion to the depth of the pacing site. A qrS pattern developed as the site of intramyocardial pacing deepened (Fig. 5F–H).

3.2. Electrograms analysis

The electrograms were classified into 6 patterns: 82 with QS patterns (16.7%), 165 with rS patterns (33.7%), 108 with qrS patterns (22.0%), 80 with qRS patterns (16.3%), 37 with rsr'S patterns (7.6%) and 18 with rsR'S patterns (3.7%). The QS pattern was recorded mainly near the insertion site of the pacing plunge electrode during subepicardial pacing (Tables 1, 2 and 3). However, it is noteworthy that a QS pattern was also often recorded during mid-myocardial pacing (Table 2); 23.1% pacing sites from which a QS pattern was recorded were at a depth of ≥ 6 mm and of these, the deepest pacing site was 8 mm deep. In contrast, an rS pattern was observed mainly during subepicardial pacing, at a horizontal distance from the insertion site of the pacing plunge electrode (Tables 1 and 3). Importantly, qrS, qRS, rsr'S or rsR'S patterns, all of which included an R-in-QR wave, were observed mainly during mid- or deep myocardial pacing, away from the site of insertion of the pacing needle, and were nearly never observed during subepicardial pacing (Tables 1, 2 and 3). Over 3/4 (76.4%) of the pacing sites associated with an R-in-QR wave were ≥ 5 mm deep (Table 2). Compared with the qrS and rsr'S patterns, the qRS and rsR'S patterns suggested a distant pacing site (Table 3).

The amplitude of the initial r of unipolar rS, rsr'S or rsR'S patterns did not correlate with the depth of the pacing site or the horizontal or linear distance between the pacing and recording sites. However, there was a weak inverse relationship between the amplitude of the Q-in-QR wave and the horizontal ($R=-0.40$; $P<0.0001$) and linear distance ($R=-0.22$; $P=0.0006$, Fig. 5A) between the pacing and the recording sites. In addition, the amplitude of the R-in-QR wave was weakly correlated with the horizontal ($R=0.25$; $P=0.0001$) and linear ($R=0.29$; $P<0.0001$; Fig. 5B) distance between the pacing and recording sites.

4. Discussion

Our study revealed the following associations between (a) morphologies of unipolar potentials and (b) the depth of their origin and distance to the recording site: (1) a QS pattern was

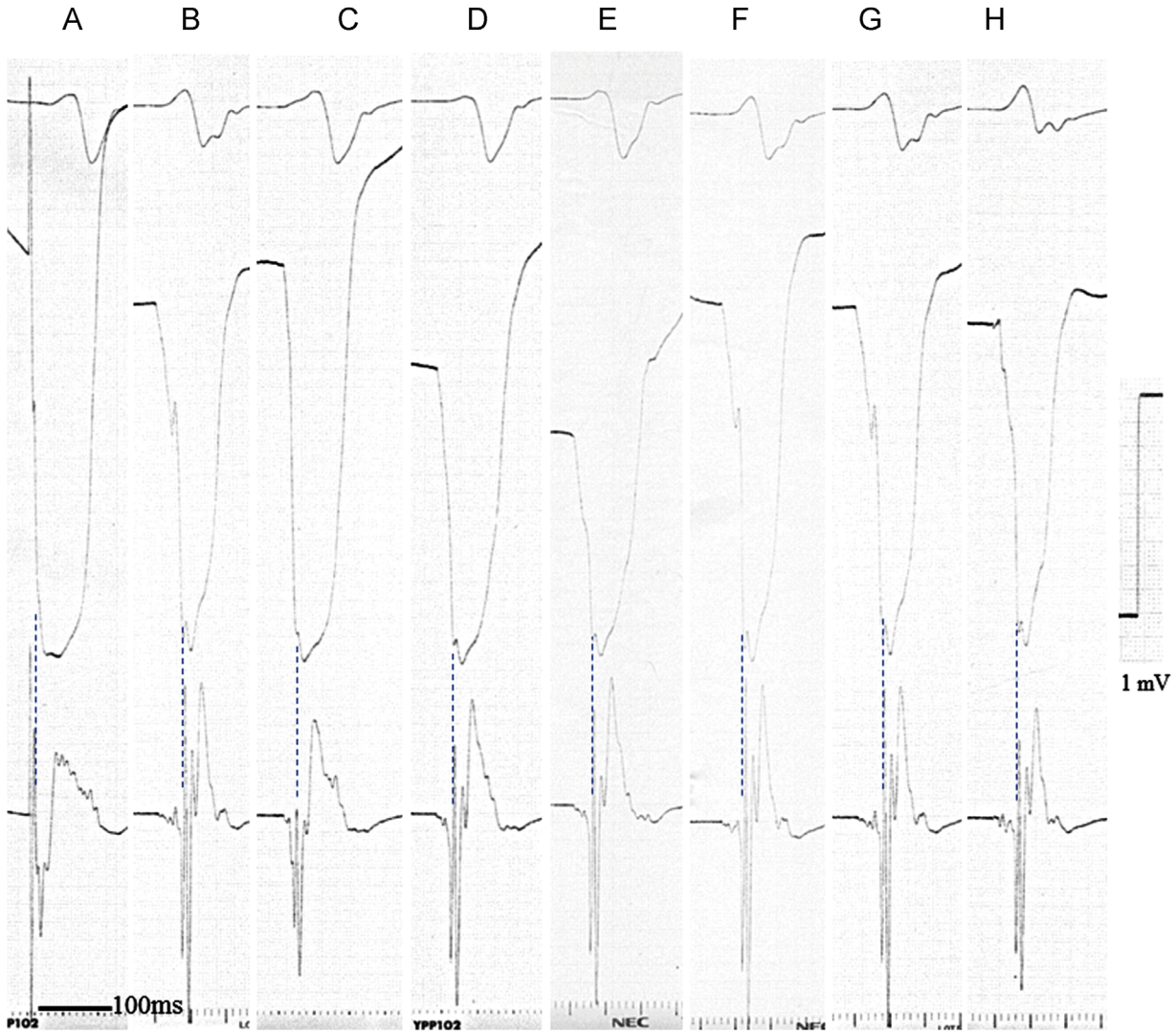

Fig. 5. Representative examples of unipolar electrograms (middle tracing) recorded at a 1-mm distance during pacing at depths of 1 (A) to 8 (H) mm. The unipolar electrograms recorded during pacing at depths of 1–5, 6–7, and 8 mm appear as QS (panels A–E), qrS (panels F to G), and rsr'S (H) complexes, respectively, along with the surface electrocardiogram (upper tracing) and the first derivatives (d*V*/d*t*) of each unipolar electrogram (lower tracing). The pacing artefact is visible at the onset of the unipolar electrograms in panels A and B. Note the absence of an initial r wave on all unipolar electrograms but H. The dashed lines indicate the timing of the minimum d*V*/d*t*. See text for further explanation.

Table 1
Depth of pacing site and horizontal and linear distances between recording sites and electrogram patterns.

Pattern (*n*)	Amplitude (mV)	Depth of pacing site (mm)	Distance between insertion and recording site (mm)	Linear distance between pacing and recording site (mm)
QS (82)	2.9 ± 0.8	3.7 ± 2.0	3.0 ± 2.7	5.1 ± 2.7
rS (165)	2.9 ± 1.7	3.2 ± 2.3	7.4 ± 2.9*	8.4 ± 3.0*
qrS (108)	3.0 ± 0.6	5.7 ± 1.6*,¶	4.1 ± 2.3¶,ϒ	7.4 ± 1.9*,¶
qRS (80)	3.0 ± 0.8	5.9 ± 1.2*,¶	6.9 ± 2.2*,#	9.3 ± 1.6*,#
rsr'S (37)	2.8 ± 2.6	5.3 ± 1.7*,¶	5.9 ± 2.9*,#,Δ	8.2 ± 2.8*
rsR'S (18)	3.1 ± 0.7	5.8 ± 0.8*,¶,#,λ,Φ	7.2 ± 1.9*,#	10.4 ± 1.2*,¶,#,Δ,ψ
All patterns	3.0 ± 1.9			

Values are means ± SD.

* $P < 0.01$ versus QS.
¶ $P < 0.01$ versus rS.
# $P < 0.01$ versus qrS.
λ $P < 0.01$ versus qRS.
Φ $P < 0.01$ versus rsr'S.
ϒ $P < 0.05$ versus QS.
Δ $P < 0.05$ versus rS.
ψ $P < 0.05$ versus rsr'S.

Table 2
Depth of the pacing site associated with each electrogram pattern.

Pattern	Depth of pacing site (mm), number (%) of electrograms							
Depth	1	2-	3-	4-	5-	6-	7-	8-
QS (n = 82)	9 (11.0)	18 (22.0)	22 (26,8)	9 (11.0)	6 (7.3)	10 (12.2)	6 (7.3)	3 (3.7)
rS (n = 165)	43 (44.2)	46 (27.9)	26 (15.8)	9 (5.5)	9 (5.5)	8 (4.8)	9 (5.5)	15 (9.1)
qrS (n = 108)	0 (0)	0 (0)	11 (10.2)	20 (18.5)	20 (18.5)	17 (15.7)	20 (18.5)	20 (18.5)
qRS (n = 80)	0 (0)	0 (0)	0 (0)	11 (13.8)	20 (25)	23 (28.8)	16 (20)	10 (12.5)
rsr'S (n = 37)	0 (0)	0 (0)	5 (13.5)	11 (29.7)	6 (16.2)	2 (5.4)	7 (18.9)	5 (1.5)
rsR'S (n = 18)	0 (0)	0 (0)	0 (0)	0 (0)	0 (0)	4 (22.2)	4 (22.2)	10 (55.6)

Table 3
Distance to the recording sites associated with each electrogram pattern.

Pattern	Distance between insertion and recording sites, number (%) of electrograms										
Depth	1-	2-	3-	4	5-	6-	7-	8-	9-	10-	10 < -
QS (n = 82)	33 (40.2)	24 (29.2)	4 (4.9)	3 (3.7)	4 (4.9)	6 (7.3)	2 (2.4)	2 (2.4)	1 (1.2)	5 (6.1)	0 (0)
rS (n = 165)	3 (1.8)	6 (3.6)	10 (6.1)	11 (6.7)	12 (7.2)	15 (9.1)	21 (12.7)	22 (13.3)	21 (12.7)	25 (15.2)	19 (11.5)
qrS (n = 108)	12 (11.1)	17 (15.7)	21 (19.4)	17 (15.7)	14 (13.0)	9 (8.3)	6 (5.6)	5 (4.6)	5 (4.6)	2 (1.9)	0 (0)
qRS (n = 80)	0 (0)	0 (0)	6 (7.5)	8 (10)	10 (12.5)	12 (15)	9 (11.3)	13 (16.3)	11 (13.8)	10 (12.5)	1 (1.3)
rsr'S (n = 37)	1 (2.7)	2 (5.4)	4 (10.8)	7 (18.9)	6 (16.2)	3 (8.1)	3 (8.1)	2 (5.4)	3 (8.1)	1 (2.7)	4 (10.8)
rsR'S (n = 18)	0 (0)	0 (0)	1 (5.6)	1 (5.6)	1 (5.6)	2 (11.1)	5 (27.8)	2 (11.1)	5 (27.8)	1 (5.6)	0 (0)

recorded when the recording was made just above a subepicardial or mid-myocardial pacing site; (2) an rS pattern was often observed when the signal was recorded away from the epicardial pacing site; (3) unique morphologies characterized by the presence of a Q-in-QR wave, followed by an R-in-QR wave, such as the qrS, qRS, rsr'S or rsR'S patterns, were observed when the recording was made just above a deep myocardial pacing site or away from a mid-myocardial pacing site; (4) the amplitude of the Q-in-QR wave was inversely correlated and that of the R-in-QR patterns was positively correlated with the horizontal and linear distance between the pacing and recording sites.

4.1. Genesis of unipolar potential morphologies

A cardiac electrogram is the product of a voltage difference between two recording electrodes. In the case of unipolar recordings, the signal from the site of recording is the positive input, whereas the reference signal, located at an infinite distance from the recording site, is the negative input. Thus, unipolar electrograms recorded from the heart reflect a global, cardiac electrical activity, although their contribution decreases with distance [16,17]. The morphology of the unipolar potential can be regarded as the sum of instantaneous current dipoles of a wave front, generating positive potentials ahead of it and negative potentials behind it (isochrones line). Moreover, in an anisotropic tissue such as the left ventricular myocardial wall, since conductivity in the horizontal direction is greater than that in the transmural direction [19], the current strength per unit length of dipole isochrone line is greater in the horizontal than in the transmural direction (Fig. 7) [20].

The genesis of typical, unipolar potential morphologies is illustrated in Fig. 7 [20]. The recording of an initial r wave at a distance of subepicardial pacing is due to the main contribution to the unipolar potential of a current dipole propagating toward that recording electrode, the strength of which exceeds the sum of current dipoles propagating away from the recording site (Fig. 7A1 and 2). As the wave front approaches the recording electrode and then propagates away from it, the deflection abruptly changes polarity, generating an rS pattern. In contrast, the absence of an initial r wave during mid- or deep myocardial pacing (Figs. 4A–J and 5A–G) despite the propagation of a wave front toward the recording site is due to the cancellation of its positive contribution by the line of negative dipoles propagating centrifugally, away from the recording site (Fig. 7B). Moreover, when the activation front approaches the recording site, the positive contribution of this line of dipoles increases due to the shortening of the distance between the line and the recording site, whereas the influence of the wave front propagating away decreases as the distance increases. Thus, a QS pattern with a gently descending slope is recorded from the mid-myocardial pacing origin (Figs. 4A and B, 5C–E, and 7B1 and 2). Importantly, when the recording was made further away from the intra-myocardial origin, such as from a deeper intra-myocardial origin or horizontally remote mid-myocardial origin, the genesis of R-in-QR wave developing after the Q-in-QR wave (Figs. 4C–J and 5F and G) is explained as follows: the positive contribution of the dipole reaching the recording site increases in proportion to the distance between the origin and the recording site while the negative contribution of the sum of dipoles propagating away from the recording site decreases because of the increasing distance. Therefore, the positive potentials are not entirely canceled by the negative potentials, resulting in a biphasic deflection (R-in-QR). Moreover, our observations suggest that because the positive contribution of the dipoles increased in proportion to the linear distance immediately before reaching the recording site, the moment at which it exceeded the sum of negative contributions was hastened, which (1) advanced the development of the R-in-QR wave that was associated with a decrease in the Q-in-QR wave amplitude, and (2) increased the amplitude of the R-in-QR wave (Fig. 6). The resulting overall morphology of the electrogram is a triphasic qrS or qRS complex.

4.2. Clinical implications

In the case of focal arrhythmias, a QS pattern is typically recorded at the site of successful catheter ablation, whereas an initial R wave is recorded away from the tachycardia origin site. The present study

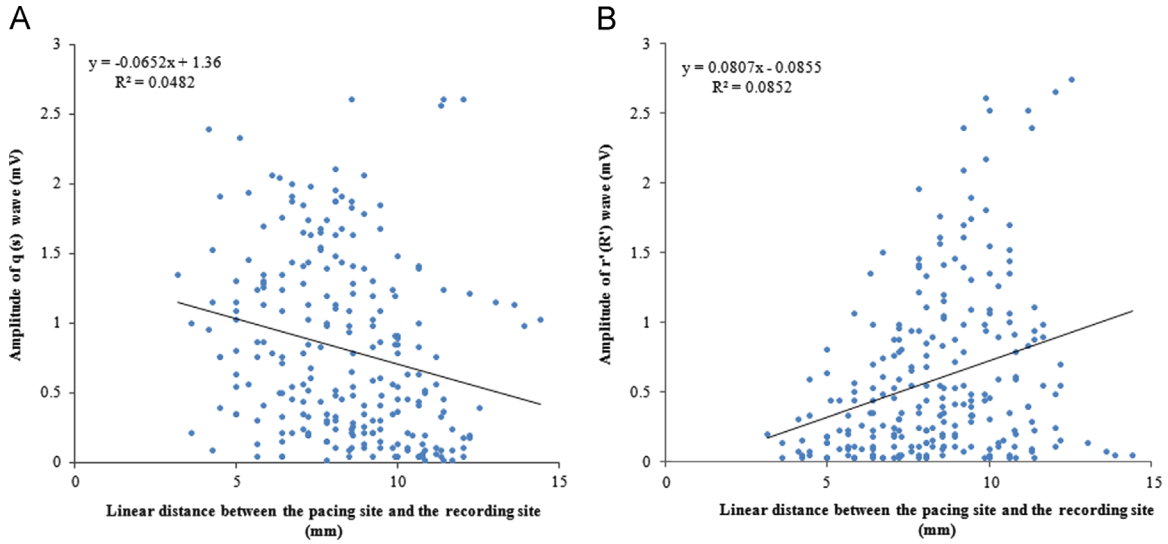

Fig. 6. Relationship between the amplitude of q wave in the qrS or qRS electrogram, including the s wave in the rsr'S or rsR'S electrogram, and the horizontal distance between the pacing and the recording sites (A) and between the amplitude of the r wave in the qrS electrogram, the R wave in qRS electrogram, the r' wave in the rsr'S electrogram, or the R' wave in the rsR'S electrogram and the linear distance between the pacing and recording sites (B).

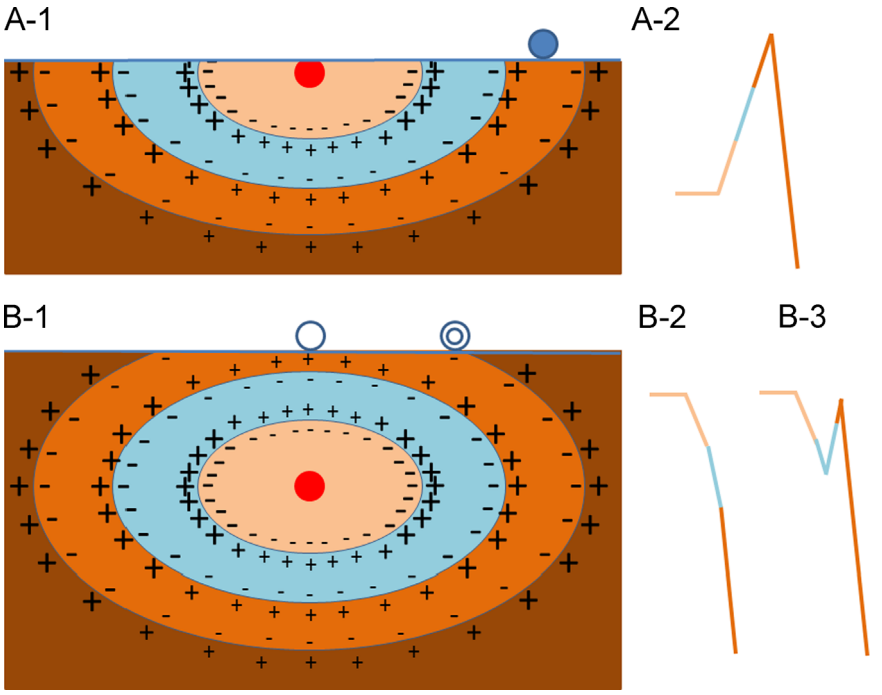

Fig. 7. Hypothetical genesis of unipolar potential morphologies based on the depth of the origin and site of recording in an anisotropic ventricular myocardium. A-1 and B-1: isochrone maps with wave front originating from the left ventricular epicardium and midmyocardium (filled red circle), respectively, and centrifugally propagating across the cream, light blue, and tan areas encircled by the adjacent isochrones lines. The current bipole corresponding to each isochrone line generates a positive potential (+) in front, and the contralateral negative potential (−) behind each isochrone line. The elliptical isochrone lines represent faster conduction in a horizontal than in a perpendicular direction. Larger positive and negative potentials in a horizontal wave front than in a perpendicular wave front are expressed as larger +or − signs. The recording site is horizontally distant from the subepicardial origin (filled circle) in panel A-1, and is immediately above (unfilled circle) and horizontally distant (double circle) from the midmyocardial origin in B-1. A-2, B-2 and B-3: Schema of the initial r wave, q wave, and the Q-in-QR wave followed by the R-in-QR wave, which are represented by segmented cream, light blue and tan lines, roughly correspond to the cream, light blue, and tan lines isochrone areas in timing, respectively.

provides new information regarding the mapping of the origin of VTAs during catheter ablation [5,8,9,10,12–15]. First, the detection of a QS pattern is not necessarily predictive of a successful ablation, since a unipolar QS electrogram is often recorded just above a deep origin that might not be affected by ablation. A shallower descending slope of the QS complex may indicate a deeper origin. Second, the presence versus absence of an initial r wave is a sensitive indicator of the distance to the activation focus, particularly when located in superficial myocardial layers, although it becomes less sensitive when the activation focus is deeper. In addition, the amplitude of the initial r wave may not be indicative of the distance to the site of origin. Finally, the detection of an R-in-QR complex during activation mapping of VTAs predicts a focal origin at a depth of $\geq$5 mm (intramural) with a sensitivity, specificity, and positive and negative predictive value approaching 75%, and a diagnostic accuracy of nearly 70%. Unlike the initial r wave, the amplitude of the R-in-QR wave is a reliable indicator of the distance to an intramural focus. The distinction of its peak below (*r* or *r*′ wave) or

above the baseline (R or R′ wave) may also be a simple estimate of the distance to its origin.

4.3. Study limitations

The first limitation of this study was the restriction of the recording area of the electrograms to within approximately 1 cm from the pacing site. Our observations should help in the identification of the earliest activation site after its approximate localization by activation mapping of bipolar potentials during VTA. Second, the genesis of endocardial unipolar potentials might be different from epicardial unipolar potentials because of differences in histology and endomyocardial versus subepicardial fiber orientation, which might influence the anisotropic conduction properties [21].

5. Conclusions

This experimental study clarified the relationships between the morphologies of unipolar electrograms and the distance and depth of their origin in the area near the origin. An rS pattern, in particular, was recorded mainly when the origin was subepicardial, and a QS pattern was also recorded with a mid-myocardial origin, whereas the presence of an R-in-QR wave following a Q-in-QR wave was indicative of an intra-myocardial origin. These observations should be helpful when recording activation maps of VTAs during catheter ablation.

Conflict of interest

The authors have no conflict of interest to disclose.

References

[1] Daniels DV, Lu YY, Morton JB, et al. Idiopathic epicardial left ventricular tachycardia originating remote from the sinus of Valsalva: electrophysiological characteristics, catheter ablation, and identification from the 12-lead electrocardiogram. Circulation 2006;113:1659–66.
[2] Jauregui Abularach ME, Campos B, Park KM, et al. Ablation of ventricular arrhythmias arising near the anterior epicardial veins from the left sinus of Valsalva region: ECG features, anatomic distance, and outcome. Heart Rhythm 2012;9:865–73.
[3] Obel OA, d'Avila A, Neuzil P, et al. Ablation of left ventricular epicardial outflow tract tachycardia from the distal great cardiac vein. J Am Coll Cardiol 2006;48:1813–7.
[4] Yokokawa M, Good E, Chugh A, et al. Intramural idiopathic ventricular arrhythmias originating in the intraventricular septum: mapping and ablation. Circ Arrhythm Electrophysiol 2012;5:258–63.
[5] Tedrow UB, Stevenson WG. Recording and interpreting unipolar electrograms to guide catheter ablation. Heart Rhythm 2011;8:791–6.
[6] Haïssaguerre M, Dartigues JF, Warin JF, et al. Electrogram patterns predictive of successful catheter ablation of accessory pathways. Value of unipolar recording mode. Circulation 1991;84:188–202.
[7] Grimm W, Miller J, Josephson ME. Successful and unsuccessful sites of radiofrequency catheter ablation of accessory atrioventricular connections. Am Heart J 1994;128:77–87.
[8] Merino JL, Jiménez-Borreguero J, Peinado R, et al. Unipolar mapping and magnetic resonance imaging of "idiopathic" right ventricular outflow tract ectopy. J Cardiovasc Electrophysiol 1998;9:84–7.
[9] Man KC, Daoud EG, Knight BP, et al. Accuracy of the unipolar electrogram for identification of the site of origin of ventricular activation. J Cardiovasc Electrophysiol 1997;8:974–9.
[10] Weiss C, Willems S, Rueppel R, et al. Electroanatomical Mapping (CARTO) of ectopic atrial tachycardia: impact of bipolar and unipolar local electrogram annotation for localization the focal origin. J Interv Card Electrophysiol 2001;5:101–77.
[11] Barlow MA, Klein GJ, Simpson CS, et al. Unipolar electrogram characteristics predictive of successful radiofrequency catheter ablation of accessory pathways. J Cardiovasc Electrophysiol 2000;11:146–54.
[12] Kusumoto FM. Unipolar recording in cardiac electrophysiologic studies. J Interv Card Electrophysiol 1999;3:121–7.
[13] Soejima Y, Aonuma K, Iesaka Y, et al. Ventricular unipolar potential in radiofrequency catheter ablation of idiopathic non-reentrant ventricular outflow tachycardia. Jpn Heart J 2004;45:749–60.
[14] Soejima Y, Iesaka Y, Aonuma K, et al. Atrial unipolar potential in radiofrequency catheter ablation of atrial tachycardia. Int Heart J 2007;48:313–22.
[15] Asso A, Pascual ED, López M, et al. Catheter ablation of repetitive monomorphic ventricular tachycardia from left ventricular outflow tract guided by unipolar mapping. J Interv Card Electrophysiol 2000;4:435–9.
[16] Blanchard SM, Damiano RJ, Asano T, et al. The effects of distant electrical events on local activation in unipolar epicardial electrograms. IEEE Trans Biomed Eng 1987;34:539–46.
[17] Damiano Jr. RJ, Blanchard SM, Asano T, et al. Effects of distant potentials on unipolar electrograms in an animal model utilizing the right ventricular isolation procedure. J Am Coll Cardiol 1988;11:1100–9.
[18] Tonkin JC, D'Alecy LG. Acute open-chest complete heart block by transeptal electrocoagulation. Am J Physiol 1990;258(5 Pt 2):H1599–602.
[19] Spach MS, Miller 3rd WT, Miller-Jones E, et al. Extracellular potentials related to intracellular action potentials during impulse conduction in anisotropic canine cardiac muscle. Circ Res 1979;45:188–204.
[20] de Bakker JMT, Hauer RNW, Simmers TA. Activation mapping: unipolar versus bipolar recording. In: Zipes DP, Jalife J, editors. Cardiac electrophysiology: from cell to bedside. 2nd ed.. Philadelphia: WB Saunders; 1995. p. 1068.
[21] Burgess MJ, Lux RL, Ershler PR, et al. Determination of transmural location of onset of activation from cardiac surface electrograms. Circulation 1990;82:1335–42.